Subproject C1.3

Synthesis and Structural Characterization of Metalloid Al and Ga Clusters

Principle Investigator: Hansgeorg Schnöckel

CFN-Financed Scientists: ….

Institut für Anorganische Chemie
Universität Karlsruhe (TH)

Synthesis and Structural Characterization of Metalloid Al and Ga Clusters

1. Preliminary Remarks

Very recently, we have prepared some reviews about metalloid Al/Ga clusters. However, in every case a special topic has been addressed:

1. Metalloid clusters and the renaissance of main group chemistry [1]
2. Metalloid clusters and the development of organometallic chemistry [2]
3. Metalloid clusters and the structure of the elements [3]
4. Structures and properties of metalloid Al and Ga clusters open our eyes to the diversity and complexity of fundamental chemical and physical processes during formation and dissolution of metals [4]

Furthermore, a comprehensive chapter in a book about molecular clusters of the main group elements has been published in 2004.[5] A further comprehensive review presenting the results up to 2008 will be published in a book about the chemistry of group 13 elements in the near future.[6] Therefore, the aim of this contribution is only to address the following recent results imbedded in the general theme of metalloid Al-Ga clusters.

2. Results

2.1 Metalloid Clusters and their Relation to Classical and Modern Inorganic Chemistry and to Zintl-like Clusters[7-10]

We have described clusters that contain both ligand-bearing and naked metal atoms that are bonded only to other metal atoms as *metalloid* or, more generally, *elementoid*, to express, in accordance with the Greek word *ειδος* (ideal, prototype), the notion that the ideal form or the motif of the solid structure of the metal or element can be recognized in the topology of the metal atoms in the cluster. The original limits of the term *metalloid*, used, for example, for the elements silicon and germanium, which are metal-like with respect to certain macroscopic properties (e.g., metallic luster), were extended to include the metalloid clusters, thus accessing an additional structural level, which can be gained only by crystal structure analysis. In general, such metalloid clusters contain more direct metal-metal contacts than metal-ligand contacts. This means that metalloid clusters represent a subgroup of the extensive metal atom cluster group in which, according to Cotton's definition, 11 nonmetal atoms may also be present, and therefore molecular clusters like $Cu_{146}Se_{73}(PPh_3)_{30}$ and similar very large clusters can be regarded as metal atom clusters, though "salt-like" clusters might be a more appropriate term. Thus, there are three different types of metal atom clusters: the naked metal atom clusters that are present under ultrahigh vacuum conditions, the metalloid clusters, which are the main subject of this review, and finally the giant "salt-like" clusters described, for example, by the groups of Fenske and Müller. The topological relations of all these types of metal atom clusters are collected and illustrated in a very recent review. Figure 1 visualizes the relation between these three types of clusters and presents a correlation with classical inorganic chemistry of the bulk phases of the metals and their salts.

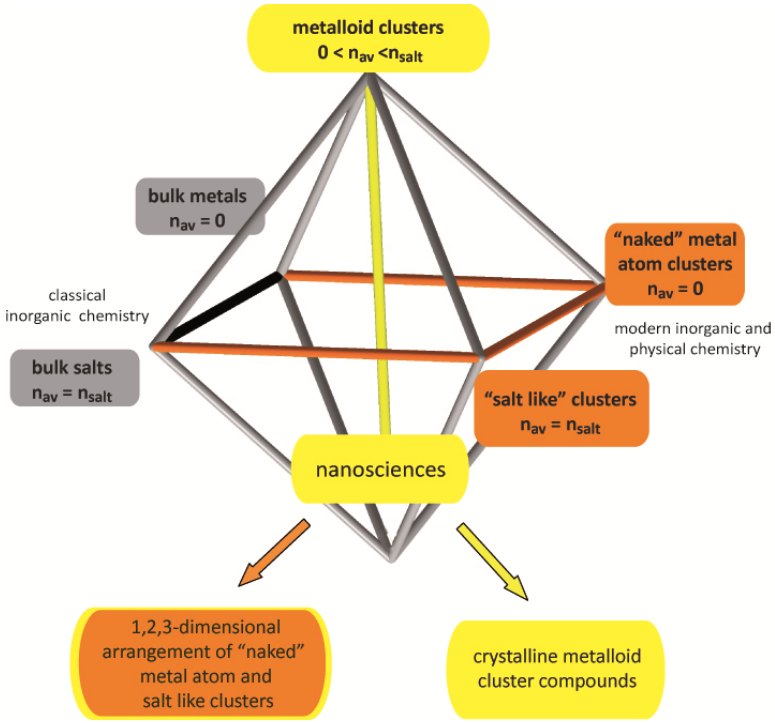

Fig 1: Interrelation between the three different types of metal atom cluster, the bulk phase of the metals and their salts, and nanosciences; n_{av} is the average oxidation state of the metal atoms.

Consequently, the three types of metal atom clusters can be regarded as intermediates of a cyclic process between the metals and their salts. The metalloid clusters represent the most complex type of cluster, because a highly mixed valence situation exists for the metal atoms, resulting in an average oxidation number between zero and the oxidation number of the salts. This falls between the much "simpler" situations of naked metal atom clusters (oxidation number 0) and the "salt-like" metal atom clusters (oxidation number *n*salt). How the three types of metal atom clusters relate to the wider field of nanoscience is also visualized in Figure 1. However, it should be mentioned that, because of the sophisticated methods needed for the preparation of metalloid clusters, the great majority of published results on nanosized metal atom clusters are based on investigations with either naked metal atom clusters or salt-like clusters.
Though the metal cluster species of Zintl ions are excluded in this contribution because the formation of metalloid molecular cluster compounds shows clear differences from that of Zintl-like phases, which have been investigated so successfully in recent years by Corbett and others, a few aspects and some recently published results should be mentioned here. Although there is a certain topological similarity to metalloid clusters, as described herein, the Zintl-like metal cluster units or the Zintl-Klemm concept. Thus, oxidation of Zintl anions proceeds by coupling of clusters toward the bulk element and via further oxidation to metalloid clusters and finally to the salt-like species. In addition, the cations located in the immediate vicinity of the anionic units lead to physical properties for these Zintl phases differing significantly from those of the molecular, ligand-protected metalloid clusters.

2.1.1 Al_4 species

In order to get a deeper feeling for the differences between these two types of cluster compounds, we extended our efforts after the detection of Al_4H_6 and during the investigations on an Al_4R_6 cluster. The $Ga_4R_4^{2-}$ cluster (Ga oxidation state +0.5) and the hypothetical Zintl-like Al_4^{2-} species

(Al oxidation state -0.5) provide two experimentally detected simple examples to make visible the similarities and differences between the chemistries of the Zintl ions (mostly stabilized in ionic solids with an overall negative oxidation state of the metal atoms) and the metalloid clusters (exhibiting oxidation states between 0 and +1). The similarities seem plausible via the bonding descriptions of Al_4^{2-} and the hypothetical $Al_4H_4^{2-}$ (Figure 2). The sequence and the shape of MOs with respect to the AlAl bonds are similar for $Al_4H_4^{2-}$ and Al_4^{2-} (Figure 2).

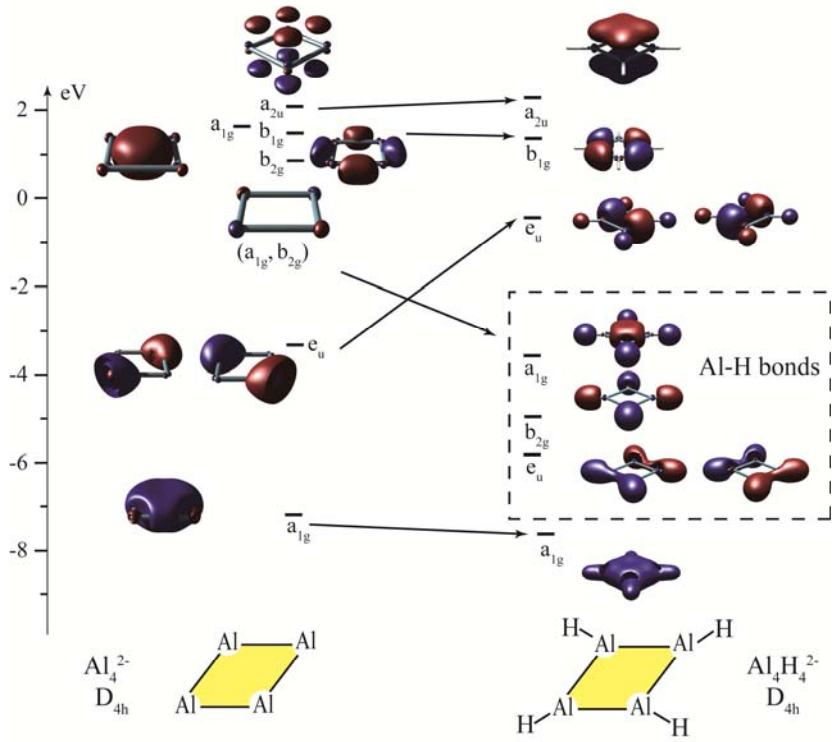

Fig 2: The MOs of Al_4^{2-} and $Al_4H_4^{2-}$ showing the HOMOs (a_{2u}) down to the HOMO-5 and HOMO-8 (a_{1g} both), respectively. The relation between the lone pairs of Al_4^{2-} and the localized AlH bonds of $Al_4H_4^{2-}$ is visible.

However, the important difference between these two species is the high energetic position of the two additional lone pairs (a_{1g} and b_{2g}) for the Zintl ion, Al_4^{2-}, in contrast to the low energy position of the four electrons localized in the four AlH bonds of $Al_4H_4^{2-}$. Therefore, it is not surprising that the calculated reaction of Al_4^{2-} with four H atoms is strongly exothermic ($\Delta E \approx$ -1300 kJ mol^{-1}). Thus, though the negative oxidation numbers in Zintl-like metalloid clusters (e.g., -0.5 in Al_4^{2-}) and the slightly positive oxidation numbers in the molecular metalloid clusters protected by bulky ligands seem to be only a formal aspect, comparison of the MOs of Al_4^{2-} and hypothetical $Al_4H_4^{2-}$ and the energy relation between these species convincingly shows the higher stability of the ligand-protected clusters, which, in accordance with the presented bonding type, can be handled in solution, even with nonpolar solvents. In contrast, Zintl clusters have a high reduction potential, with a negative unprotected charge on the surface of the ions, causing a high reactivity (e.g., the strong association with positively charged species in any equilibrium solution). Thus, though there are similarities between Zintl ions and metalloid clusters with respect to bonding between the metal atoms, there are not only formal differences (oxidation number) but also differences in principle between the two kinds of metalloid clusters. Consequently, it seems to be a highly ambitious challenge for further investigations to stabilize "naked" pure Al_n^- cluster ions such as the Al_4^{2-} anion and the prototypical jellium cluster Al_{13}^- as salt-like compounds. Therefore, supported by the abovementioned stabilization via ligand bonding, the chance to observe clusters of this kind

experimentally, for example, as crystalline compounds, increases in going from Al_4^{2-} to $Al_4H_4^{2-}$ /$Al_4R_4^{2-}$, and finally to the Al_4H_6/Al_4R_6 molecules, which have been investigated under mass spectrometric conditions (Al_4H_6) and as a crystalline substance (Al_4R_6) Fig 3.

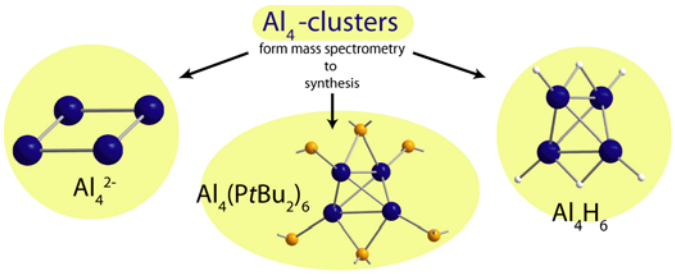

Fig 3. The relation between the gaseous species Al_4^{2-} and Al_4H_6 and the crystalline compound Al_4R_6.

That is, stability increases via step by step oxidation. To summarize, bonding in the field of low-valent Al and Ga compounds is a very complex and diverse subject, even for species containing M_4 moieties. The unexpected stability islands for molecules like Al_4H_6 and Al_4R_6 provide further insight into novel bonding.

An appropriate description of Al_4H_6 /Al_4R_6 starts from the hypothetical species $Al_4H_4^{2-}$ (Figure 3). This *planar*- molecule with its four 2e2cAl-Al bonds and one occupied π orbital is energetically stabilized by about 300 kJ mol^{-1} relative to the tetrahedral isomer. An additional stabilization results if two H^+ ions approach an $Al_4H_4^{2-}$ moiety. Consequently a distortion via the diagonals of the square molecule results, generating Al_4H_6 as a D_{2d}-shaped molecule in which the H atoms are integrated into the bonding of the whole cluster. The high stability of Al_4H_6 is evident from the highly exothermic reaction of two H^+ ions with an $Al_4H_4^{2-}$ anion: even after subtraction of the Coulomb attractions, the value $\Delta E \approx$ -1500 kJ mol^{-1} is obtained.

2.1.2. Al_{12} cluster

The missing link between the two types of clusters (Zintl versus metalloid) makes both experimental (e.g. thermodynamic) and theoretical investigations highly challenging. Therefore we have prepared a crystalline, molecular Al_{12} cluster compound that may help solve this fundamental problem, and which may be called a hybrid between a metalloid cluster and a hypothetical molecular Zintl phase. DFT calculations based on experimentally determined thermodynamic and structural data support this idea.

The relation between these Al_{12} metalloid clusters on the one hand and Zintl/Wade clusters (a molecular $Al_{12}K_8$ Zintl phase?) and the Wade type $Al_{12}R_{12}^{2-}$ and the metalloid $Al_{12}R_8^-$ radical on the other hand; is visualized on the title picture of Angewandte Chemie (Figure 4).

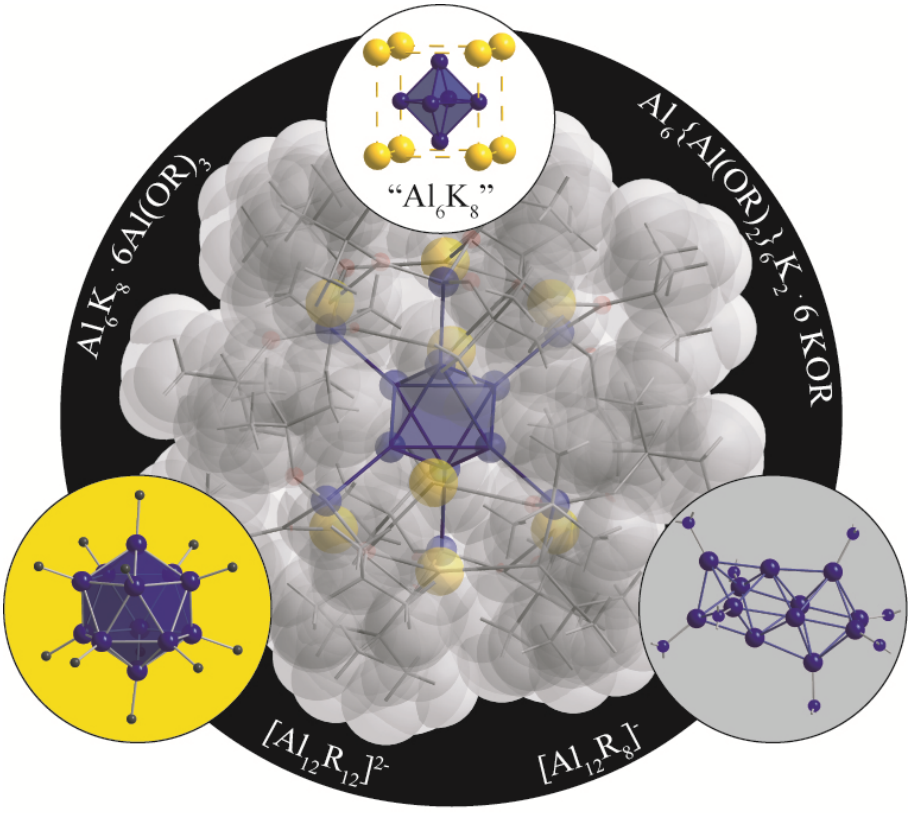

Fig 4: The novel Al_{12} cluster $[Al_6\{Al(OR)_2\}_6K_2 \cdot 6\ KOR]$ in the center and its relation to other Al_{12} species and the hypothetical Al_6K_8 Zintl molecule (Cover picture Angew. Chem. Int. Ed. **49,** 3146 (2010)).

The bonding in this Al_{12} cluster becomes clearer when the following model clusters (with OR groups substituted by chloro ligands) are discussed with the help of DFT calculations: $[Al_{12}Cl_{12}]^{2-}$ **2**, $[Al_{12}Cl_{12}K_2]$ **2'**, $[Al_6Cl_6]^{2-}$, $[Al_6]^{8-}$, $[Al_6(AlCl_2)_6]^{2-}$ **3**, $[Al_6(AlCl_2)_6K_2]$ **3'**, and Al_6K_8 **4**. Although the structural data of the clusters under discussion (and even the Al-K distances) are more or less similar, there is a drastic electronic difference between the icosahedral $K_2[Al_{12}Cl_{12}]$ cluster **2'** and the Al_6K_8 species **4** and all the other clusters; only these two clusters have calculated ^{27}Al NMR values that are shifted heavily to low-field in the direction of the Knight shift: **2'**458 ppm, **4** 482 ppm.[11,41–44] On the basis of these NMR data, it is evident that the Zintl-type and Wade-type bonding in **2** and 4 is different from the bonding in metalloid clusters. Therefore, the molecular compound **1'** (^{27}Al NMR: 168, 148 ppm) may be described more adequately as a metalloid cluster $[Al_6(AlCl_2)_6]K_2 \cdot 6$ KCl than a Zintl phase-like cluster $[Al_6K_8 \cdot 6AlCl_3]$, with the Wade/Zintl-type typical bonding properties of molecular moiety Al_6K_8 4 suppressed by the complexation of the six $AlCl_3$ units. To confirm our interpretation, thermodynamic calculations were carried out (Figure 5). The starting point corresponds to the experimental chemistry with $12AlCl_{(g)}+2K_{(g)}+6KCl_{(g)}$. The disproportionation reaction to the gaseous species $8Al+4AlCl_3+2K+6KCl$ experimentally is endothermic (916 kJ) and in accordance with the calculated value (919 kJ).

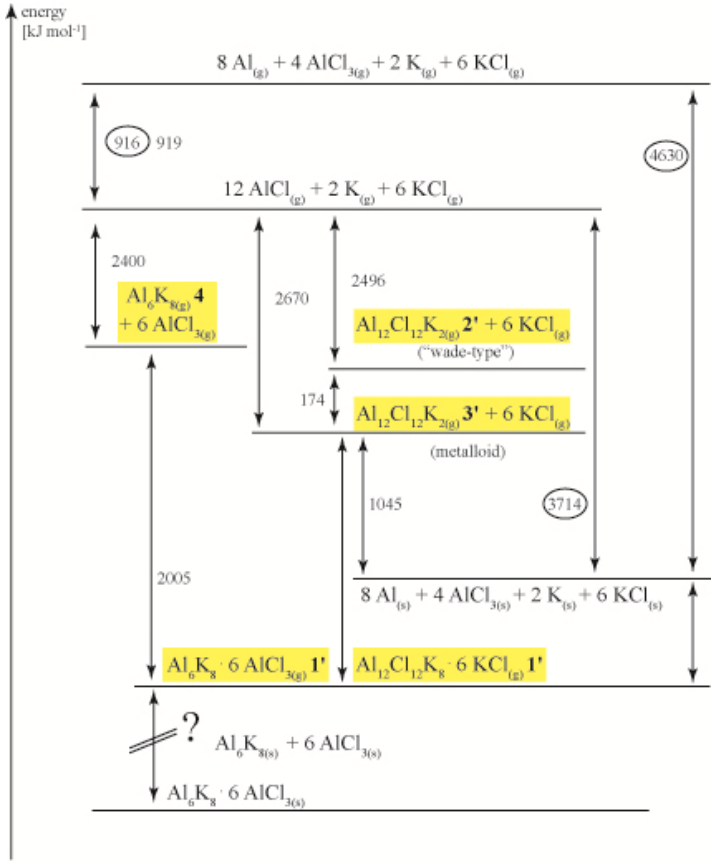

Fig 5: The energetic relation (kJ mol^{-1}) between the hypothetical highlighted Al_6/Al_{12} clusters $Al_{12}Cl_{12}K_2$ (**2'**), $Al_6(AlCl_2)_6K_2$ (**3'**), Al_6K_8 (**4**), and $[Al_6(AlCl_2)_6]K_2 \cdot 6KCl$ / $[Al_6K_8 \cdot 6AlCl_3]$ **1'**. The experimentally based energy values are marked by circles.

The formation from the AlCl level of both $[Al_{12}Cl_{12}]K_2$ clusters (**2'** and **3'**) is strongly exothermic: metalloid cluster **3'** 2670 kJ, icosahedral Wade-type cluster **2'**2496 kJ. The metalloid isomer **3'** is thus favored by 174 kJ, and the metalloid cluster **3'** is favored in comparison to the molecular Zintl phase **4** by 270 kJ; that is, **3'** is exothermically formed by a comproportionation reaction from **4** and $AlCl_3$. The thermodynamic data presented herein thus show that there is a fluent energetic change between both types of clusters (Zintl/Wade and metalloid). However, even before the complexation by six $AlCl_3$ or six KCl molecules, the metalloid cluster **3'** is preferred in comparison to **2'** and **4**. Therefore it is not surprising that also after the complexation the metalloid character in gaseous **1'** is still present. This bonding type is also expected in solid **1'**; however, on the way to solid **1'**, the solid Zintl phase Al_6K_8 4 with a non-metalloid (Wade-type) bonding has to be addressed as an intermediate. Furthermore, all results presented herein show that the oxidation number of the aluminum atoms n provides an impressive though formal description of the different cluster types: n=-1.3 for **4**, n=+0.3/+3 for **1'**, and n=0.83 for **2**. Perhaps this result may be the starting point for investigations to a novel unified concept for the description of bonding within the entire field of metal-to-metal atom clusters.

After the discussion of the formation and bonding of $Al_4(PR_2)_6$ and the Al_{12} clusters via disproportionation reactions an alternative channel of the decomposition of Al(I) (PR_2) species will be presented. The failure to form phosphanide-substituted Al clusters, in contrast to the generation of similar Ga clusters and analogous Al amide clusters, was the starting point of this contribution. For aluminum(I) phosphanides, there exists a different decomposition route in which the saltlike bulk material AlP and not Al metal is the final product Fig 6 (cf. Fig 1).

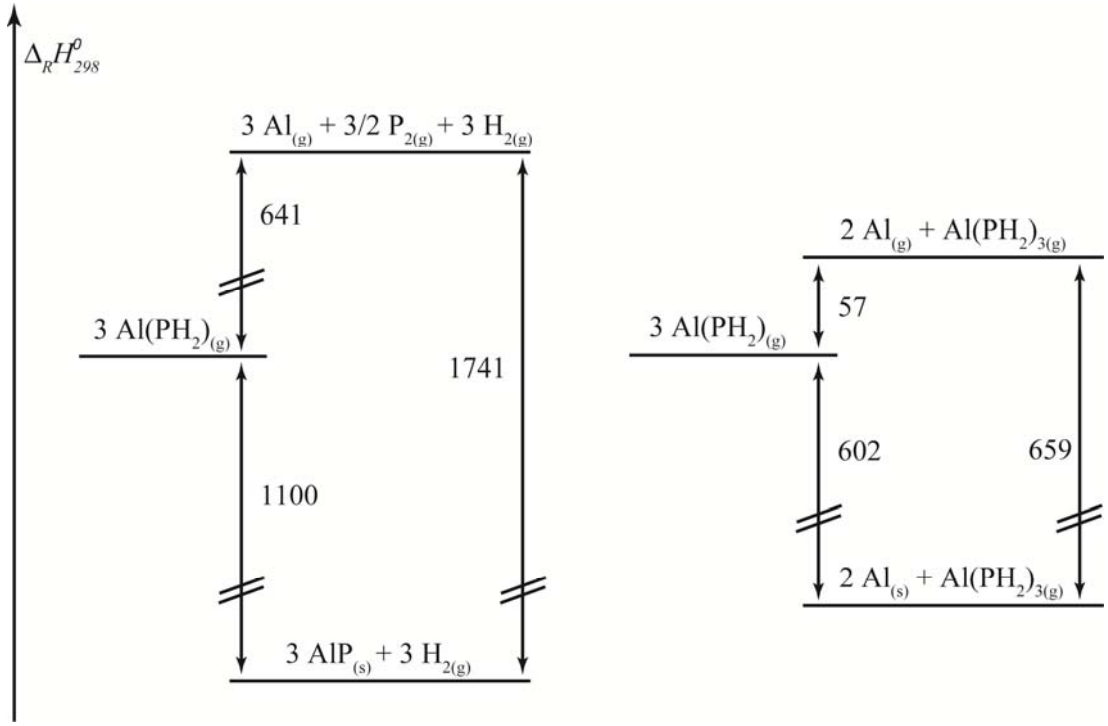

Fig 6: Calculated ΔH values for the two decomposition routes of $Al(PH_2)$: to bulk AlP and H_2 (left); to bulk Al metal and $Al(PH_2)_3$ (right).

The synthesis of two molecular "AlP" intermediate species, $(Al_8Br_8(P^tBu_2)_6$ and $Al_3(P^tBu_2)_4Cl_2$, together with supporting DFT calculations, provide plausible arguments for this decomposition route, which is thermodynamically favored for many AlR/GaR species and which, surprisingly, has not been discussed before.

2.2 Reactions of the Al_{13}^- Cluster as a Model for the Dissolution of Bulk Al [11-14]

The size dependence of the stability and reactivity of metal clusters and its possible relation to reactive processes of bulk metals is an active topic of research. In particular, aluminum clusters recently attracted attention due to their peculiar combination of electronic and structural properties. The resulting reactivity patterns, e.g., shed a new light on the possible role of spin conservation in cluster reactions and also led to the idea of so called superatoms. In the latter context, reactions of aluminum clusters with halogen-containing compounds were of special interest. While reactant and product properties of these reactions have been characterized in some detail, mechanistic information and kinetic data are scarce.

Despite the principal differences between the chlorination of Al_{13}^- and of Al metal, that is, only a few reaction steps versus a complex reaction cascade, a surprising similarity emerges, at least with respect to the thermodynamics of the reactions (eqs 1 and 259):

$Al_{13}^-{}_{(g)} + 3Cl_{2(g)} = Al_{11}^-{}_{(g)} + 2AlCl_{3(g)}$ $\quad \Delta_R H$ =-1137 kJ mol^{-1} (calculated) (1)

$2Al_{(s)} + 3Cl_{2(g)} = 2AlCl_{3(g)}$ $\quad \Delta_R H$ = -1166 kJ mol^{-1} (exptl. found) (2)

Since this similarity of thermodynamic properties applies only to the Al_{13}^- cluster, the very special electronic structure of this cluster (jellium model), as well as its highly symmetric arrangement (i.e., a double magic behavior) with a topological similarity to the bulk metal, is critical. Recently we have presented a time-resolved experimental study of the $Al_{13}^-+Cl_2$ reaction system and have shown that the degradation kinetics observed can be described by a reaction sequence:

$$Al_n^- + Cl_2 \rightarrow Al_nCl_2^-$$
$$Al_nCl_2^- \rightarrow Al_nCl + Cl^-$$
$$Al_nCl_2^- \rightarrow Al_{n-1}Cl^- + AlCl$$
$$Al_{n-1}Cl^- \rightarrow Al_{n-1} + Cl^-$$
$$Al_{n-1}Cl^- \rightarrow Al_{n-2}^- + AlCl$$

with n=13, 11, 9, and 7. We deduce kinetic parameters and discuss these values in terms of results from statistical rate theory with molecular properties from quantum chemical calculations. The kinetics of the Aln^- intermediates in the reaction sequence arising from the Al_{13}^-+Cl_2 reaction can be explained in terms of association-elimination reactions, where the association reactions occur with a rate near the Langevin limit. Statistical rate theory calculations show that the experimentally observed degradation in double steps is likely to be due to a sequential elimination of two AlCl molecules from the highly excited adduct clusters, for which average lifetimes have been calculated. To account for the observed Cl^- formation, however, parallel charge-transfer/abstraction channels bypassing the association steps have to be assumed. Kinetic parameters for the channel branchings were inferred. The general aspects of the mechanism, that is, the competition of unimolecular dissociation steps producing $AlCl^-$ and finally $AlCl_3$ in excess of Cl_2 at higher pressures and consecutive bimolecular reactions cluster +Cl_2 can be included in future quantitative kinetic models of aluminum oxidation in a Cl_2 atmosphere. Analogous competing reactions may also be important for metal oxidation processes in general.

Besides this and former detailed studies on the reactivity of Al_{13}^- anions [12, 13, 15] we cooperated with the group of Prof. Kit H. Bowen, John Hopkins University, Baltimore, in the following investigation of Al_n cluster reactions:

1. All Al_n^- cluster anions react with TDMAE molecules (tetrakis(dimethylamino)ethylene) in the identical way. The Al_n^- cluster anions eliminate one Al- atom which inserts into the C-N bond of TDMAE to form the $[Al(TDMAE)]^-$ anion.

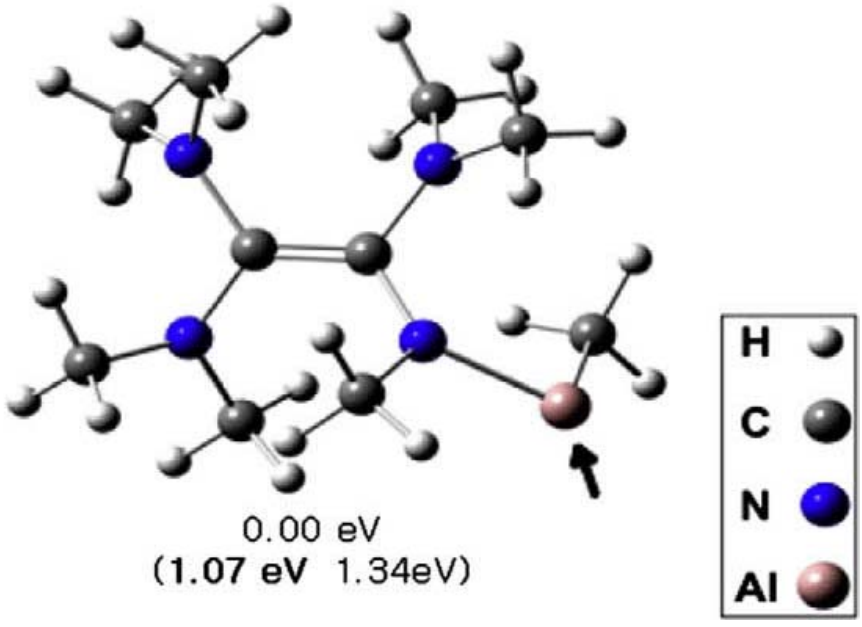

Fig 7: Calculated structure of the most stable $[Al(TDMAE)]^-$ isomer. (VDE and EA_a)

No Al_n^- clusters containing the TDMAE moiety are observed.

2. The reactivity of Al_n^- clusters with ammonia has been studied via mass spectrometry. Selective etching of Al_{11}^- and Al_{12}^- was observed upon exposure of aluminum cluster anions to moderate ammonia concentrations. $Al_{11}NH_3^-$ and $Al_{12}NH_3^-$ species each with a chemisorbed ammonia molecule were identified as the main reaction products. A two-step reaction mechanism was proposed, wherein an NH_3 molecule initially physisorbs onto the cluster and subsequently chemisorbs by forming a relatively strong Al–N bond. The conversion from the physisorbed precursor into the chemisorbed adduct is proposed as the rate-determining step. The putative barrier may stem from the need to flip the NH_3 molecule from its energetically more favorable orientation with H atoms facing the negatively charged cluster in the physisorbed species into one, where the N atom faces the cluster in the chemisorbed adduct. The following order of barrier heights was inferred from the observed reactivity patterns: $Al_{12}^- < Al_{11}^- << Al_{n<11}^- < Al_{n<13}^- << Al_{13}^-$. Thus, it appears that varying barrier heights govern the selective etching observed in this work. Lastly, it is interesting to speculate that such barriers are likely to be much smaller in the case of neutral clusters or even entirely absent in the case of positively charged clusters, where orientation of the ammonia molecule is likely to be the same in the physisorbed and chemisorbed states.

3. Using a combination of anion photoelectron spectroscopy and density functional theory calculations, the influence of the shell model on H atom site selectivity in $Al_{13}H^-$ was explored. Photoelectron spectra revealed that $Al_{13}H^-$ has two anionic isomers and for both of them provided vertical detachment energies (VDEs). Theoretical calculations found that the structures of these anionic isomers differ by the position of the hydrogen atom. In one, the hydrogen atom is radially bonded (lower energy), while in the other, hydrogen caps a triangular face.

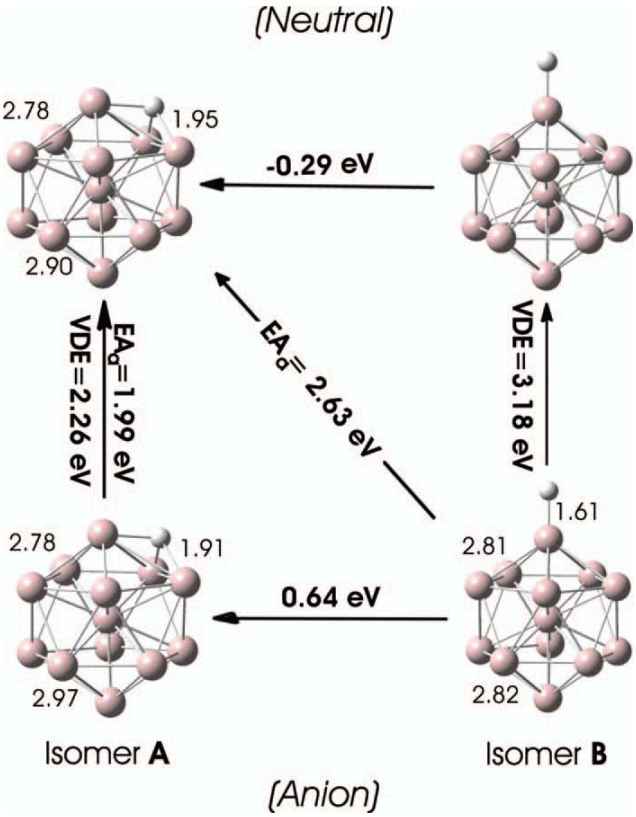

Fig 8: Calculated lowest energy structures of both isomers of anionic $Al_{13}H^-$ and neutral $Al_{13}H$ along with their calculated energetic relationships.

VDEs for both anionic isomers as well as other energetic relationships were also calculated. Comparison of the measured versus calculated VDE values permitted the structure of each isomer to be confirmed and correlated with its observed photoelectron spectrum. Shell model, electron-

counting considerations correctly predicted the relative stabilities of the anionic isomers and identified the stable structure of neutral $Al_{13}H$.

2.3 Metalloid Al and Ga Clusters as Intermediates on the Way from the Salts to the Metals [16-18]

Before the presentation of a Ga_8Br_8 species as a nanoscaled step on the way to the bulk modification of β-Ga (2.3.2) and the unexpected property of an Al_{50} cluster to prevent the decomposition of the textbook molecule $Al_4Cp^*_4$ (2.3.3) the primary step of any metal cluster formation will be presented (2.3.1).

2.3.1

The formation of an AlAl-σ bond is the first essential step during the formation of any Al_nR_m cluster. Therefore, we have investigated this fundamental reaction as a prototype of any σ-bond formation. The results for the $[Al_2(PR_2)_4]$ compounds extend the area of intermediates of σ-bond-formation processes by contributing additional structurally characterized snapshots (visualized in a cover picture of Angew. Chem. Int. Ed. 2009, 48, 8141; Figure 9). For the first time, a particularly large distance between two metal centers was investigated in a biradical species, which, after several further steps, finally leads to a σ-bond. This unprecedented discovery was only possible owing to the particularly mild reaction conditions present in metastable AlX/AlR solutions. These mixtures show a complex disproportionation behavior, which is marked by several other intermediates that have already been characterized finally forming the metal and AlX_3. Apparently, the $\{Al_2P_4\}$ ring system under study is particularly suited for such investigations because its Al-Al σ bond is weak, yet still strong enough to compete with the bridging Al-P bonds.

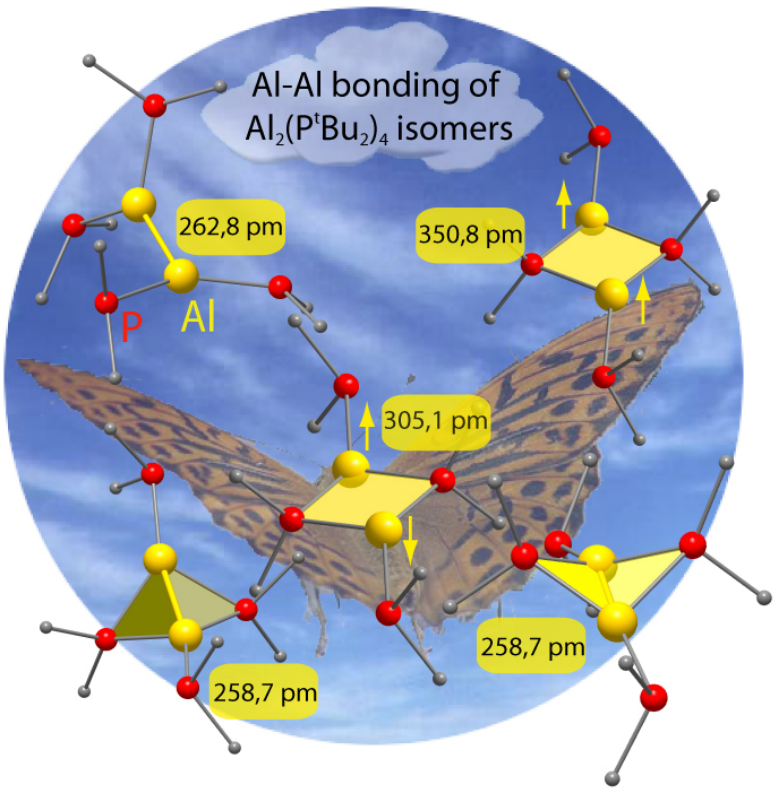

Fig 9: Cover picture Angew. Chem. Int. Ed. **48**, 8141 (2009) exhibiting the formation of AlAl bonds of Al_2R_4 isomers.

2.3.2.

Because of their thermodynamic instability, their sophisticated formation, and their high reactivity, only three textbook examples of Al(I)/Ga(I) subhalides have been crystallized so far: Al_4Br_4, Al_4I_4, and Ga_8I_8. In contrast, the recently published $Ga_{10}Br_{10}$ molecule represents a highly mixed valent subhalide: $Ga_4(GaBr)_2(GaBr_2)_4$ (Figure 10).

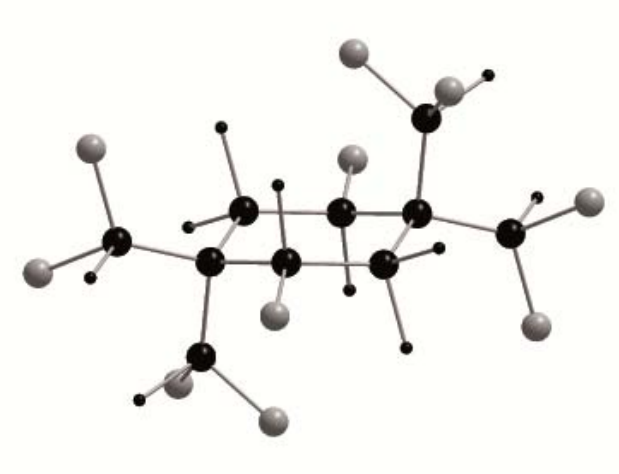

Fig 10: The molecular structure of donor stabilized $Ga_{10}Br_{10}$.

Here, we present the formation and structural characterization of molecular Ga_8Br_8 species. (J. Am. Chem. Soc. 2010,132, 1323) The different structures of Ga_8I_8 and Ga_8Br_8 are discussed with regard to their different formation conditions and their different thermodynamic stability based on results from DFT calculations. Structural as well as thermodynamic properties of Ga_8I_8 and Ga_8Br_8 are strongly related to the low-temperature modifications β-Ga and γ-Ga.

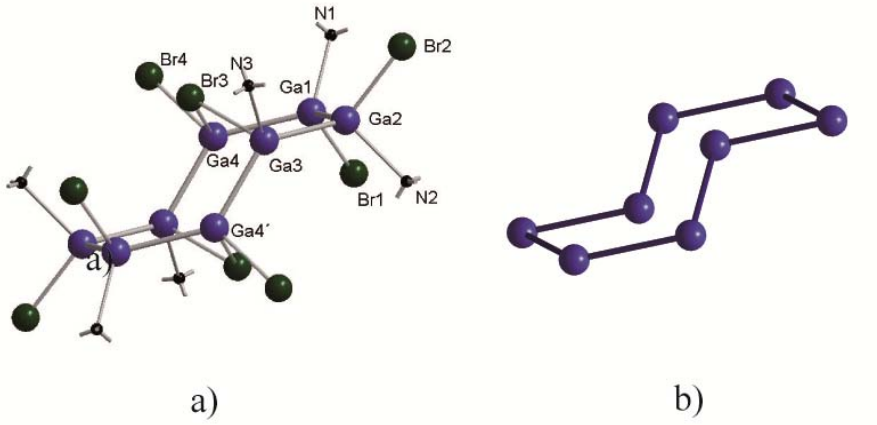

Fig 11: The molecular structure of donor stabilized Ga_8Br_8 (a) and similar Ga_8 moiety of the β-gallium (b).

Therefore, our fruitful hypothesis about the fundamental relation between structure and energy of a number of metalloid clusters and the corresponding element modifications is now supported by two binary Ga(I)-halide compounds.

2.3.3

The stability of $[Al_4Cp^*_4]$ ($Cp^*=C_5Me_5$) **1** has been investigated, mainly as tetrameric entities in solution and in the solid state. The dissociation of the tetramers to monomeric units in solution and in the gas phase at 100 °C (the temperature of the classical synthesis) has also been investigated. However, the fact that the disproportionation of **1** is hindered, even above 100 °C, has never been discussed, which is surprising because the unsubstituted analogue $[Al_4Cp_4]$ ($Cp=C_5H_5$) (**2**) spontaneously decomposes to metallic aluminum and Al^{III} species even when it is warmed to temperatures above -30 °C. The lack of discussion of these observations is especially surprising because the tetramerization energy of [AlCp] (191 $kJmol^{-1}$) is larger than that of $[AlCp^*]$ (160 $kJmol^{-1}$). What are the reasons for these discrepancies, which may be crucial for many metastable subvalent organometallic compounds? Here we present an answer: Metalloid clusters such as the $[Al_{50}Cp^*_{12}]$ cluster represent a barrier as intermediates on the way to the formation of metals, that is, clusters of this type may also be assigned as experimentally characterized nuclei for the crystallization of metals, which means that these investigations are of fundamental interest in the chemistry of any metastable organometallic compound as well as in solid-state chemistry. To quantify the relationship between the calculated gas-phase species and the final formation of the bulk metal, the DFT results have been adjusted with the vaporization energy of Al to obtain a suitable thermodynamic ladder. The results obtained for **1** and **2** are presented in Figure 12.

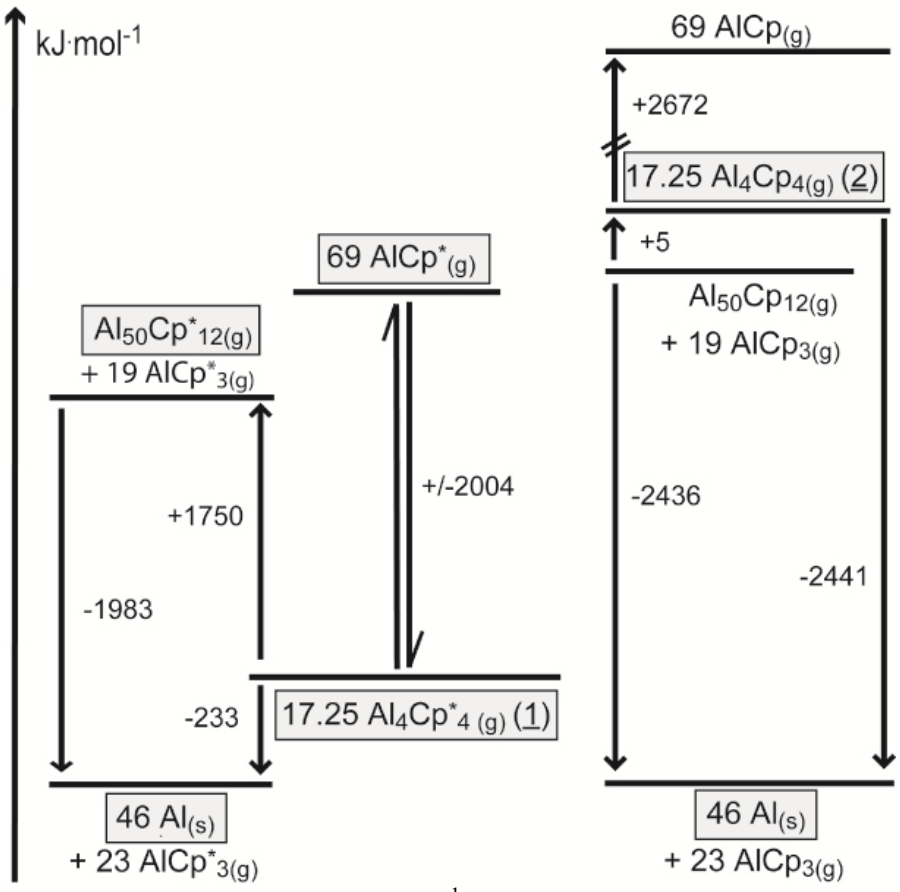

Fig 12: Calculated energy diagram ($kJ·mol^{-1}$) of the monomerization of $Al_4Cp^*_4$ **1** and Al_4Cp_4 **2** and of the disproportionation reaction of **1** and **2** via $Al_{50}R_{12}$ clusters to solid Al and AlR_3 molecules. The experimentally detected species are highlighted. The formation of $Al_4Cp^*_8/Al_4Cp_8$ together with $AlCp^*_3/AlCp_3$ corresponding to eq. 1 is 941 kJ above the $Al_4Cp^*_4$ and 84 kJ below the Al_4Cp_4 level.

The following points are remarkable:

1) Both compounds (**1** and **2**) are metastable with respect to disproportionation. However, the exothermic dissociation energy of 233 kJ/17.25 mol for **1** is dramatically smaller than that of **2** (2441 kJ/17.25 mol).
2) There is a high energy barrier of about 1750 kJ for the disproportionation of **1** via $[Al_{50}Cp^*_{12}]$ clusters, whereas there is nearly no barrier via a similar $[Al_{50}Cp_{12}]$ cluster for the disproportionation of **2**. This is in accordance with the observation that only **2** can decompose to metallic aluminum and Al^{III} species spontaneously.
3) Since **1** does not disproportionate during heating and dissociation to the monomers (+2004 kJ), the above-mentioned barrier via $[Al_{50}Cp^*_{12}]$ can easily be reached by repeated addition of monomeric $AlCp^*$ to undissociated **1** and subsequent $[AlCp^*_3]$ elimination. Snapshots on this pathway are $[Al_8Cp^*_4]$, $[Al_{20}Cp^*_8X_{10}]$, and $[Al_{50}Cp^*_{12}]$. However, the Al_{50} cluster should not mark the peak of the barrier, since the central Al_8 unit has not grown to the expected Al_{13} core, which should be the typical core of any nucleus of the crystallization of metallic Al; that is, the top of the barrier may be a metalloid cluster a little bit larger than $[Al_{50}Cp^*_{12}]$.

Therefore, the results presented herein demonstrate that the essential contribution of metalloid clusters to many fields of chemistry may be the starting point for many theoretical papers, since, for example, the number of subvalent organometallic compounds has considerably increased over the last two decades.

2.4 From Matrixisolated Magnesium(I) halides to a Preparative Scale[19, 20]

After the first evidence for stable alkaline earth(I) halides were shown to be erroneous about 50 years ago, about 40 years ago the first ESR spectroscopic evidence was given for MgF, among other examples, as a gaseous molecule at a temperature of 2300 °C trapped in an inert-gas matrix. For this purpose, MgF_2 was vaporized at about 1250 °C; subsequently, the gaseous MgF_2 molecules were dissociated to MgF and F atoms at about 2350 °C. To find a feasible synthesis technique in analogy to the synthesis of AlCl at approximately 900 °C, there should be no further component (e.g. Mg(g)) in the equilibrium composition besides gaseous MgCl and $MgCl_2$, otherwise the entropically favored formation of monohalides would be put at risk. In contrast to the entropically favored endothermic formation of AlCl ($Al(l)+AlCl_3(g)\rightarrow 3AlCl(g)$), the Mg vapor pressure is already 1.5 mbar at 800 °C; thus, we looked for a solid magnesium-containing compound with a significantly reduced Mg activity; for example, with a low decomposition pressure. We chose MgB_2, a well-known compound with unexpected superconducting capabilities, as its Mg partial pressure had been examined in detail and amounts to not more than 10^{-3} mbar at 800 °C.
In principle, the following reactions to produce $MgCl_2$ and MgCl could take place when HCl is passed over heated MgB_2[Eq. (1), (2)].

$$MgB_2(s) + 2\,HCl(g) = H_2(g) + 2\,MgCl(g) + 4\,B(s) \qquad (1)$$

$$MgB_2(s) + 2\,HCl(g) = H_2 + MgCl_2(g) + 2\,B(s) \qquad (2)$$

The subtraction of Equation (2) from Equation (1) yields the relevant components for the equilibrium presented in Equation (3).

$$MgB_2(s) + MgCl_2(g) = 2\,MgCl(g) + 2\,B(s) \qquad (3)$$

Finally, supported by several experiments on the thermal stability of MgB_2 as well as by quantum-chemical calculations on MgCl and Mg_2Cl_2, the temperature-dependent partial pressure curves of $MgCl_2$, MgCl, and Mg_2Cl_2 are obtained and experimental investigations have been started:
When HCl is passed over MgB_2 at approximately 700 °C and when this gas phase, together with a large surplus of inert gas (N_2, Ar), is trapped on a copper surface cooled to 10 K, the Raman spectrum of MgCl, $MgCl_2$ and Mg_2Cl_2 results.

Since the substitution of Mg_2Cl_2 by bulky ligands has been calculated to be exothermic; i.e. a suitable method for a novel Mg(I) chemistry may be provided, we started first experiments to synthesis metastable solutions of MgX at -78 °C which subsequently should react via salt elimination e.g. with $LiCp^*$, KCp^*, $LiPR_2$ and $KN(SiMe_3)_2$. Since the Mg(I) solutions exhibit a high tendency to disproportionate even at low temperatures (above -60 °C) where the substitution reaction does not proceed, we have to increase the reactivity for the substitution reaction e.g. via crown ethers and PMDTA to coordinate lithium/potassium cations. Using KCp^* activated by 18-crown-6 ether we obtained, in a repetitive way, black crystals. However, up to now it was not possible to determine the structure of these crystals.
With other salts like LiP^tBu_2 and $KN(SiMe_3)_2$ results of metathesis reactions with magnesium monohalides are also promising; i.e. in the reactions with LiP^tBu_2 we probably obtain neutral products because extremely good solubility in pentane is observed. All attempts to obtain the already known dimeric magnesium $Dipp_2$nacnac complex as the first example containing an MgMg single bond[21] using the alternative reaction between MgCl and $Dipp_2$nacnacLi were unsuccessful so far.

Though all attempts to crystallize an Mg(I) compound failed there are strong hints for such species e.g. via EPR spectra many reaction products exhibit the expected radical character. Furthermore ongoing experiments using α-diimine ligands are also promising to confirm the presence of MgX species in the original solutions: MgCl solution reacts with DAB-Dipp to the following diradical species characterized via EPR spectroscopy and its structure determination (Fig. 13).[22]

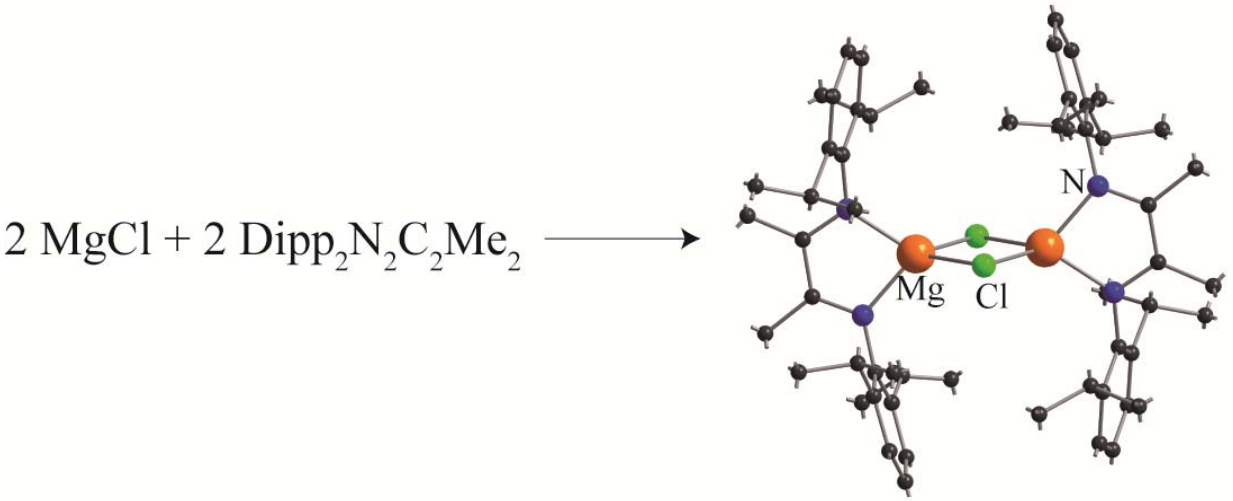

Fig 13: The reaction of two MgCl radicals to the diradicalic $Mg_2Cl_2(DAB\text{-}Dipp)_2$ molecule

To sum up, we are optimistic to open a new field of magnesium chemistry between normal valent Mg compounds and the bulk metal i.e. in the area of nanoscaled species via some exciting results in the near future.

References

[1] H. Schnöckel, *Formation, structure and bonding of metalloid Al and Ga clusters. A challenge for chemical efforts in nanosciences*, Dalton Trans. 4344 (2008)
[2] H. Schnöckel, *Metalloid Al- and Ga-clusters: a novel dimension in organometallic chemistry linking the molecular and the solid-state areas?*, Dalton Trans. 3131 (2005)
[3] A. Schnepf, H. Schnöckel, *Metalloid aluminum and gallium clusters: Element modifications on the molecular scale?*, Angew. Chem., Int. Ed. **41** 3532 (2002)
[4] H. Schnöckel, *Structures and Properties of Metalloid Al and Ga Clusters Open Our Eyes to the Diversity and Complexity of Fundamental Chemical and Physical Processes during Formation and Dissolution of Metal*, Chem. Rev. **110** 4125 (2010)
[5] G. Linti, H. Schnöckel, W. Uhl, N. Wiberg, in *Molecular Clusters of the Main Group Elements* (Eds.: M. Drieß and H. Nöth), Wiley-VCH, Weinheim, **2004**, pp. 126
[6] A. Schnepf, H. Schnöckel, in *Chemistry of the Group 13 Metals Al, Ga, In and Tl Revisited* (Eds.: S. Aldridge and A. J. Downs), Wiley-VCH, Weinheim, Germany, **in preparation**
[7] X. Li, A. Grubisic, S. T. Stokes, J. Cordes, G. F. Ganteför, K. H. Bowen, B. Kiran, M. Willis, P. Jena, R. Burgert, H. Schnöckel, *Unexpected Stability of Al_4H_6: A Borane Analog?*, Science **315** 356 (2007)
[8] P. Henke, M. Huber, J. Steiner, K. Bowen, B. Eichhorn, H. Schnöckel, *$Al_4(PtBu_2)_6$ - a Derivative of Al_4H_6 - and Other Al_4 Species: A Challenge for Bonding Interpretation between Zintl Ions and Metalloid Clusters*, J. Am. Chem. Soc. **131** 5698 (2009)
[9] P. Henke, N. Trapp, C. E. Anson, H. Schnöckel, *$Al_{12}K_8\{OC(CH_3)_3\}_{18}$: A Wade, Zintl, or Metalloid Cluster, or a Hybrid of All Three?*, Angew. Chem., Int. Ed. **49** 3146 (2010)
[10] P. Henke, H. Schnöckel, *Metastable Aluminum(I) Compounds: Experimental and Quantum Chemical Investigations on Aluminum(I) Phosphanides-An Alternative Channel to the Disproportionation Reaction?*, Chem. A Eur. J. **15** 13391 (2009)
[11] M. Olzmann, R. Burgert, H. Schnöckel, *On the kinetics of the $Al_{13}^-+Cl_2$ reaction: Cluster degradation in consecutive steps*, J. Chem. Phys. **131** 174304 (2009)
[12] R. Burgert, H. Schnöckel, M. Olzmann, K. H. Bowen, *The chlorination of the $[Al_{13}]^-$ cluster and the stepwise formation of its intermediate products, $[Al_{11}]^-$, $[Al_9]^-$, and $[Al_7]^-$: a model reaction for the oxidation of metals?*, Angew. Chem., Int. Ed. **45** 1476 (2006)
[13] R. Burgert, S. T. Stokes, K. H. Bowen, H. Schnöckel, *Primary Reaction Steps of Al_{13}^- Clusters in an HCl Atmosphere: Snapshots of the Dissolution of a Base Metal*, J. Am. Chem. Soc. **128** 7904 (2006)
[14] A. Grubisic, X. Li, S. T. Stokes, K. Vetter, G. F. Ganteför, K. H. Bowen, P. Jena, B. Kiran, R. Burgert, H. Schnöckel, *Al_{13}^-: hydrogen atom site selectivity and the shell model*, J. Chem. Phys. 121103 (4) (2009)
[15] R. Burgert, H. Schnöckel, A. Grubisic, X. Li, S. T. Stokes, K. H. Bowen, G. F. Ganteför, B. Kiran, P. Jena, *Spin Conservation Accounts for Aluminum Cluster Anion Reactivity Pattern with O_2*, Science **319** 438 (2008)
[16] P. Henke, T. Pankewitz, W. Klopper, F. Breher, H. Schnöckel, *Snapshots of the Al-Al sigma-Bond Formation Starting from {AlR2} Units: Experimental and Computational Observations*, Angew. Chem. Int. Ed. **48** 8141 (2009)
[17] T. Duan, P. Henke, G. Stößer, Q. F. Zhang, H. Schnöckel, *$Ga_8Br_8{\cdot}6NEt_3$: Formation and Structure of Donor-Stabilized GaBr. A Nanoscaled Step on the Way to beta-Gallium?*, J. Am. Chem. Soc. **132** 1323 (2010)
[18] M. Huber, P. Henke, H. Schnöckel, *Experimentally Based DFT Calculations on the Hindered Disproportionation of $Al_4Cp^*_4$: Formation of Metalloid Clusters as Intermediates on the*

Way to Solid Al Prevents the Decomposition of a Textbook Molecule, Chem A Eur. J. **15** 12180 (2009)
[19] T. Pankewitz, W. Klopper, P. Henke, H. Schnöckel, *Isomeric Al_2R_4, Mg_2R_2 Species and Oligomerisation Products: Investigation of Al-Al and Mg-Mg sigma Bonding*, Eur. J. Inorg. Chem. 4879 (2008)
[20] R. Köppe, P. Henke, H. Schnöckel, *MgCl and Mg_2Cl_2: From Theoretical and Thermodynamic Considerations to Spectroscopy and Chemistry of Species with Mg-Mg Bonds*, Angew. Chem., Int. Ed. **47** 8740 (2008)
[21] S. P. Green, C. Jones, A. Stasch, Science **318** 1754 (2007)
[22] P. Henke, H. Schnöckel, in preparation